

https://doi.org/10.1070/QEL16320

Efficient two-dimensional sub-wavelength atom localisation via probe absorption in a four-level Λ-shaped atomic system

M. Sahrai, F. Bozorgzadeh

Abstract. **Two-dimensional (2D) atom localisation of a four-level Λ-shaped atomic system with a nearly hyper-fine doublet interacting with two orthogonal standing-wave fields is investigated. The spatial information of a moving atom in *xy* plane is obtained by measuring the probe field absorption. The effect of quantum interference on two-dimensional atom localisation is described. The intensity of standing-waves and the detuning of the probe and standing-wave fields are found to strongly affect the two-dimensional atom localisation that lead to different spatial distribution patterns.**

Keywords: *atom localisation, absorption, sub-wavelength, susceptibility.*

1. Introduction

In recent years, studying the atomic position in the sub-wavelength domain has attracted much attention due to its potential application in nanolithography [1], laser cooling [2], Bose–Einstein condensation [3], etc. Quantum interference arising from atomic coherence is an important mechanism to determine the atomic position through the standing-wave field. One important method for measuring the position of a moving atom is detection of the spontaneously emitted photon by the atom when it passes through the standing-wave field. Qamar et al. [4, 5] investigated the methods for acquiring precise information about the position of two-level [4] and three-level [5] atoms moving through a standing-wave field by measuring the spontaneously emitted photon's frequency. They found that four localisation peaks with equal probability in the unit wavelength domain of the classical standing-wave field can be obtained. The spatial position of the moving atom will then strongly depend on the relative phase of applied fields, which reduces the periodicity of the system by 2 due to the quenching of the spontaneous emission [6]. This increases the probability of finding the atom at a particular position by a factor of 2 just by controlling the relative phase of applied fields. An important advantage of such sub-wavelength atom localisation, based on the measurement of the spontaneously emitted photon's frequency, is the determination of the atomic position within the sub-wavelength domain during its motion through the standing-wave field. However, in these schemes, not only the atom should be prepared in the upper level, but also the spontaneously emitted photon should be detected, which is not practical for experimental implantation. Paspalakis et al. [7] showed that atom localisation can also be achieved via the measurement of the population in upper level of a Λ-type atomic system. For a weak probe field, they observed that the measurement of the population in upper level leads to sub-wavelength atom localisation during its motion through standing-wave fields. In our work [8–10], we showed that the position of a moving atom through the standing-wave field can be determined by the measurement of probe field absorption frequency. In fact, electromagnetically induced transparency [11] has opened up a new route for sub-wavelength atom localisation, which may allow better localisation with the same conventional measurement resolution. The basic idea is that the measurement of probe field absorption at appropriate frequencies localises the moving atom inside the classical standing-wave field. Thus, the position of the atom along the standing-wave field is determined as the probe field absorption frequency is measured. In this case, the atom would be in its ground state that is easy to implement. We have shown that for a certain choice of controlling parameters, such as the relative phase of driving fields, one can confine the atom to one of the half-wavelength regions. Therefore, two localisation peaks occur in one of the half-wavelength regions. This new domain of atom localisation is called sub-half-wavelength localisation [10]. Thus, probe absorption peaks are restricted to one-half of each wavelength, which results in better atom localisation with the same conventional measurement resolution based on measurement of absorption frequency. The effect of quantum interference arising from spontaneously generated coherence (SGC) [12] has also been taken into account in sub-half-wavelength atom localisation [13]. It has been found that the effect of the SGC makes the probe absorption phase dependent. It has also been shown that measurement of a certain probe field frequency leads to sub-wavelength atom localisation in either of the two half-wavelength regions by an appropriate choice of the phase difference between applied fields [13].

On the other hand, two-dimensional (2D) atom localisation has been discussed with respect to the measured spontaneously emitted photon [14], quantum interference [15], interacting double-dark resonances [14, 16], population of upper levels [17] and probe field absorption [18–20]. The precise position of the atom in the two-dimensional *xy* plane was determined via the measurement of the upper level population by Ivanov et al. [17]. A scheme of two-dimensional atom localisation based on phase-sensitive probe field absorption was proposed in a four-level atomic system with an assisting radio-frequency (RF) driven field [18]. In this case, 2D atom

M. Sahrai, F. Bozorgzadeh Research Institute for Applied Physics and Astronomy, University of Tabriz, Tabriz, Iran;
e-mail: sahrai@tabrizu.ac.ir

Received 14 February 2018; revision received 20 October 2018
Kvantovaya Elektronika **49** (3) 220–225 (2019)
Submitted in English

localisation patterns are obtained in the sub-wavelength domain of the standing-wave. Furthermore, the behaviour of two-dimensional atom localisation in a N-type tripod five-level atomic system driven by two orthogonal standing-wave fields was also investigated [20]. In another proposal, Qamar [21] discussed the two-dimensional atom localisation via probe field absorption in a three-level Λ-type atomic system when the atom interacts with a weak probe and two orthogonal standing-wave fields. The double-dark resonance in a four-level double-Λ configuration was studied by Shapiro [22]. The conditions for coherent population trapping were calculated when a nonabsorbing superposition of upper states was formed in a four-level double-Λ system.

We investigate the two-dimensional atom localisation in a four-level atomic system with a nearly hyper-fine doublet of closely spaced upper levels. We examine the response of probe field absorption when the atomic system interacts with two orthogonal standing-wave fields. The quantum interference effect is employed to reach the precise position of the atom by measuring the weak probe field absorption. The spatial information of the atom through two-dimensional standing-wave fields strongly depends on the probe field detuning. An appropriate probe field detuning leads to the highly precise detection of the position in a sub-wavelength region of standing-waves. The effect of the frequency detuning of two standing-wave fields and their intensities on two-dimensional atom localisation is also discussed.

2. Model and density-matrix equations of motion

Consider a closed four-level atomic system coupled by two laser fields (Fig. 1a). The atomic system includes a nearly hyper-fine doublet of closely spaced levels $|3\rangle$ and $|4\rangle$ with a frequency difference $\omega_{34} = 2\Delta$, where $\Delta = (\omega_4 - \omega_3)/2$. Two-dimensional standing-wave fields of frequency ω_c couple level $|2\rangle$ to levels $|3\rangle$, $|4\rangle$, while a weak probe laser field of frequency ω_p applies to the transition $|1\rangle \leftrightarrow |3\rangle(|4\rangle)$. The spontaneous decay rates from upper levels $|3\rangle$ and $|4\rangle$ to lower levels $|2\rangle$ and $|1\rangle$ are defined as $\gamma_{32(31)}$ and $\gamma_{42(41)}$, respectively. We assume that the centre-of-mass position of the atom is nearly constant along the direction of the standing-wave, and the atom moves along the z axis and passes through the intersection region of two classical standing-waves fields, as shown in Fig. 1b. Hence, we apply the Raman–Nath approximation and neglect the kinetic energy term of the Hamiltonian. The interaction Hamiltonian of the system is given by

$$H = \sum_{j=1}^{4} E_j |i\rangle\langle j| - \hbar\Omega_c \exp(-i\omega_c t)\,|3\rangle\langle 2| - \hbar\Omega_c \exp(-i\omega_c t)\,|4\rangle\langle 2|$$

$$- \hbar\Omega_p \exp(-i\omega_p t)\,|3\rangle\langle 1| - \hbar\Omega_p \exp(-i\omega_p t)\,|4\rangle\langle 1| + \text{H.C.}, \qquad (1)$$

where $E_j = \hbar\omega_j$ is the energy of the levels $|j\rangle$ ($j = 1,2,3,4$); $\Omega_p = \Omega_{31(41)} = \mu_{31(41)}\varepsilon_p/(2\hbar)$ is the Rabi-frequency of the weak probe laser field that drives the transition $|1\rangle \leftrightarrow |3\rangle(|4\rangle)$; $\Omega_c(x,y) = \Omega_{xy}[\sin(kx) + \sin(ky)]$ is the position dependent Rabi-frequency of two orthogonal standing-wave fields that drives the transition $|2\rangle \leftrightarrow |3\rangle(|4\rangle)$; $\Omega_{xy} = \Omega_{32(42)} = \mu_{32(42)}\varepsilon_c/(2\hbar)$; $\mu_{31(41)}$ and $\mu_{32(42)}$ are the corresponding electric dipole moments; and ε_c and ε_p are the amplitudes of the two coherent standing-wave fields and a weak probe laser field, respectively. Under the rotating wave approximation, the density matrix equations of motion can be written in the form [23]

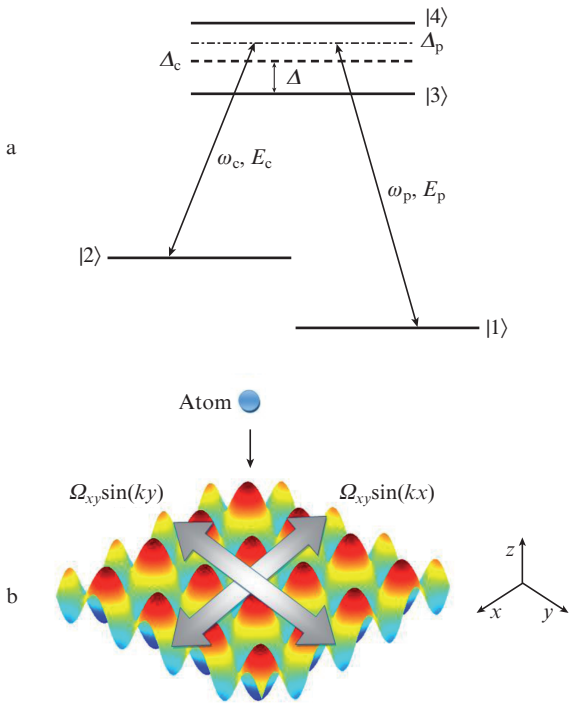

Figure 1. (a) Four level Λ-type atomic system: two orthogonal standing-wave fields couple upper levels $|3\rangle$ and $|4\rangle$ to $|2\rangle$ and a weak tunable probe field couples level $|1\rangle$ to both levels $|3\rangle$ and $|4\rangle$; and (b) schematic diagram for the two dimensional localisation of an atom.

$$\dot\rho_{44} = i\Omega_c(\rho_{24} - \rho_{42}) + i\Omega_p(\rho_{14} - \rho_{41})$$
$$- 2(\gamma_{14} + \gamma_{42})\rho_{44} - (\eta_1 + \eta_2)(\rho_{43} + \rho_{34}),$$
$$\dot\rho_{33} = i\Omega_c(\rho_{23} - \rho_{32}) + i\Omega_p(\rho_{13} - \rho_{31})$$
$$- 2(\gamma_{31} + \gamma_{32})\rho_{33} - (\eta_1 + \eta_2)(\rho_{43} + \rho_{34}),$$
$$\dot\rho_{43} = -(\gamma_{41} + \gamma_{42} + \gamma_{31} + \gamma_{32} + i2\Delta)\rho_{43} + i\Omega_c(\rho_{23} - \rho_{24})$$
$$+ i\Omega_p(\rho_{13} - \rho_{41}) - (\eta_1 + \eta_2)(\rho_{44} + \rho_{33}),$$
$$\dot\rho_{42} = -[\gamma_{41} + \gamma_{42} + i(\Delta - \Delta_c)]\rho_{42} + i\Omega_p\rho_{12}$$
$$- i\Omega_c(\rho_{43} + \rho_{44} + \rho_{22}) - (\eta_1 + \eta_2)\rho_{32}, \qquad (2)$$
$$\dot\rho_{41} = -[\gamma_{41} + \gamma_{42} + i(\Delta - \Delta_p)]\rho_{41} + i\Omega_c\rho_{21}$$
$$- i\Omega_p(\rho_{43} + \rho_{44} + \rho_{11}) - (\eta_1 + \eta_2)\rho_{31},$$
$$\dot\rho_{32} = -[\gamma_{31} + \gamma_{32} + i(\Delta - \Delta_c)]\rho_{32} + i\Omega_p\rho_{12}$$
$$- i\Omega_c(\rho_{34} + \rho_{33} - \rho_{22}) - (\eta_1 + \eta_2)\rho_{42},$$
$$\dot\rho_{31} = -[\gamma_{31} + \gamma_{32} - i(\Delta + \Delta_p)]\rho_{31} + i\Omega_c\rho_{21}$$
$$- i\Omega_p(\rho_{34} + \rho_{33} - \rho_{11}) - (\eta_1 + \eta_2)\rho_{41},$$
$$\dot\rho_{21} = -i(\Delta_c - \Delta_p)\rho_{21} + i\Omega_c(\rho_{31} + \rho_{41}) - i\Omega_p(\rho_{23} + \rho_{24}).$$

Here, $\Delta_c = \omega_c - \omega_0$ and $\Delta_p = \omega_p - \omega_0$ are the detunings between applied fields and the corresponding atomic transitions; and

$\omega_0 = (\omega_3 + \omega_4)/2$. The parameters $\eta_1 = \sqrt{\gamma_{41}\gamma_{31}}\cos\theta_1$ and $\eta_2 = \sqrt{\gamma_{42}\gamma_{32}}\cos\theta_2$ describe the effect of quantum interference between two decay pathways, $|4\rangle(|3\rangle) \rightarrow |1\rangle$ and $|4\rangle(|3\rangle) \rightarrow |2\rangle$. In fact, quantum interference arises due to the decay from two upper levels $|3\rangle$ and $|4\rangle$ to level $|1\rangle$ or level $|2\rangle$. Here, $\cos\theta_1 = \boldsymbol{\mu}_{41}\boldsymbol{\mu}_{31}/(\mu_{41}\mu_{31})$ [or $\cos\theta_2 = \boldsymbol{\mu}_{42}\boldsymbol{\mu}_{32}/(\mu_{42}\mu_{32})$] represents the alignments of the corresponding electric dipole moments. If the two dipole moments become parallel or anti-parallel, i.e. $\theta_1 = \theta_2 = 0(\pi)$, quantum interference becomes maximal. But if the electric dipole moments are perpendicular to each other, i.e. $\theta_1 = \theta_2 = \pi/2$, then quantum interference is minimal, i.e. $\eta_1 = \eta_2 = 0$. We assume the atom to be initially in its ground level $|1\rangle$, so that $\rho_{11}^{(0)} = 1$ and $\rho_{ij}^{(0)} = 0$ $(i, j = 1, 2, 3, 4)$.

After linearisation, the necessary equations from the set of density matrix elements are given by

$$\begin{aligned}
\dot{\rho}_{31} &= -[\gamma_{31} + \gamma_{32} - \mathrm{i}(\Delta + \Delta_\mathrm{p})]\rho_{31} + \mathrm{i}\Omega_\mathrm{c}\rho_{21} \\
&\quad + \mathrm{i}\Omega_\mathrm{p} - (\eta_1 + \eta_2)\rho_{41}, \\
\dot{\rho}_{41} &= -[\gamma_{41} + \gamma_{42} + \mathrm{i}(\Delta - \Delta_\mathrm{p})]\rho_{41} + \mathrm{i}\Omega_\mathrm{c}\rho_{21} \\
&\quad + \mathrm{i}\Omega_\mathrm{p} - (\eta_1 + \eta_2)\rho_{31}, \\
\dot{\rho}_{21} &= -\mathrm{i}(\Delta_\mathrm{c} - \Delta_\mathrm{p})\rho_{21} + \mathrm{i}\Omega_\mathrm{c}(\rho_{31} + \rho_{41}).
\end{aligned} \tag{3}$$

By solving equations (3) in the steady state, i.e. $\dot{\rho}_{ij} = 0$, we obtain the density matrix elements ρ_{31} and ρ_{41}

$$\begin{aligned}
\rho_{31}^{(1)} &= \frac{-\mathrm{i}\Omega_\mathrm{p}}{\det M}\{\mathrm{i}(\Delta_\mathrm{c} - \Delta_\mathrm{p})[\gamma_{41} + \gamma_{42} + \mathrm{i}(\Delta - \Delta_\mathrm{p})] + (\eta_1 + \eta_2)\}, \\
\rho_{41}^{(1)} &= \frac{-\mathrm{i}\Omega_\mathrm{p}}{\det M}\{\mathrm{i}(\Delta_\mathrm{c} - \Delta_\mathrm{p})[\gamma_{31} + \gamma_{32} - \mathrm{i}(\Delta + \Delta_\mathrm{p})] + (\eta_1 + \eta_2)\},
\end{aligned} \tag{4}$$

where M is a matrix of the density matrix coefficients in equations (3). The observable quantity is the electric susceptibility as a response of the atomic medium to the applied fields. Thus, the linear susceptibility can be written as [23]

$$\chi = \frac{2N}{\varepsilon_0\varepsilon_\mathrm{p}}(\mu_{12}\rho_{31} + \mu_{14}\rho_{41}), \tag{5}$$

where N is the number of injected atoms to the interaction region. Generally, the linear susceptibility is a complex quantity that is defined as $\chi = \chi' + \mathrm{i}\chi''$. The real part of χ corresponds to the dispersion, while the imaginary part indicates the probe field absorption. In fact, the imaginary part of χ'' i.e. absorption, is our main point of interest in discussing the probe field absorption along the standing-wave fields.

Equation (5) implies that the linear susceptibility is characterised by the coherence term ρ_{31} and ρ_{41}. It is obvious that the imaginary parts of susceptibility depend on the position dependent Rabi-frequency, the detuning of two orthogonal standing-wave fields and probe field detuning, and on the quantum interference effect. Thus, the problem reduces to the measurement of the position-dependent probe field frequency that provides information about the atomic position.

Note that atom localisation means the measurement of the conditional position probability of the atom moving inside the pre-defined wavelength domain. In fact, the peak position of the probe absorption profile shows where the atom is localised. Then, the number of peaks in one sub-wavelength domain indicates the detection probability, and the width of the peak shows the localisation precision [24].

3. Results and discussion

In order to achieve high precision 2D atom localisation, we investigate the imaginary part of equation (5) to discuss the information about the position of an atom moving inside the two-orthogonal standing-wave laser fields. From the analytical solutions given in equations (4) and (5), it is obvious that the probe absorption depends on the intensity of two-orthogonal standing-wave fields and the detuning of probe and standing-wave fields. Also, quantum interferences arising from two spontaneous decay channels, i.e. $|4\rangle(|3\rangle) \rightarrow |1\rangle$ and $|4\rangle(|3\rangle) \rightarrow |2\rangle$, have a crucial role on position-dependent probe field absorption. Thus, an atom can be localised in the specific positions on the xy plane by proper measurement of probe field frequency. We assume that $\gamma_{41} = \gamma_{31} = \gamma_{42} = \gamma_{32} = \gamma$ and all the other parameters are scaled by γ.

Figure 2 shows the two-dimensional probe absorption for various values of the standing-wave field detuning Δ_c. Figures 2a, 2c and 2e show the results in absence of quantum interference, while Figs 2b, 2d and 2f – in its presence. If $\Delta_\mathrm{c} = 0$, the probe absorption is distributed in two quadrants of the xy plane (Fig. 2a), which has the 'cross' structure pattern in second and fourth quadrants. By gradually increasing Δ_c to the value of 20γ, the 'cross' pattern of the probe absorption become wider and the accuracy of the two-dimensional atom localisation will be reduced. Physically, with increasing Δ_c, the resonance condition in the system is disturbed, and this leads to atomic decoherence. Therefore, the position of the atom cannot be determined with high precision. Figures 2b, 2d and 2f illustrate the effect of quantum interferences, i.e. $\eta_1 = \eta_2 = 1$, on the spatial distribution of the probe absorption. It is found that the spatial distribution of the imaginary part of the susceptibility is initially located in all quadrants of the xy plane, where probe absorption has a cross-like pattern in second and fourth quadrants, but it has a spherical pattern in first and third quadrants. With increasing Δ_c, these spherical patterns will fade away. Comparing Figs 2e and 2f shows that for the off-resonance condition the effect of quantum interferences vanish.

A remarkable result can be found in Fig. 3, where the effect of the probe field detuning on probe absorption is investigated. One can see from Figs 3a and 3b that the imaginary part of the susceptibility has a cross-like pattern. But with increasing Δ_p, interesting localisation patterns start to appear. According to Fig. 3c, in the absence of quantum interference, probe absorption exhibits a crater-like pattern in the first and third quadrants, and this leads to the localisation of the atom at the circular edges of these craters. Furthermore, with increasing Δ_p to 30γ, the spatial distribution of the atom localisation shows a spike-like pattern, as plotted in Figs 3e and 3f. In such a case, high-precision and high-resolution 2D atom localisation is obtained. This is to say that the atom is localised with a high precision position in a sub-wavelength region of standing-waves with a spike-like pattern in the positions $(kx, ky) = (\pi/2, \pi/2)$ and $(kx, ky) = (-\pi/2, -\pi/2)$. These interesting localisation patterns can be used for enhancing the capability of many existing devices, such as optical microscopy, atom imaging, measurement of the centre-of-mass wave function of moving atoms, trapping of neutral atoms, etc.

Figures 3b, 3d and 3f show the effect of quantum interferences on the atom localisation for various probe field detun-

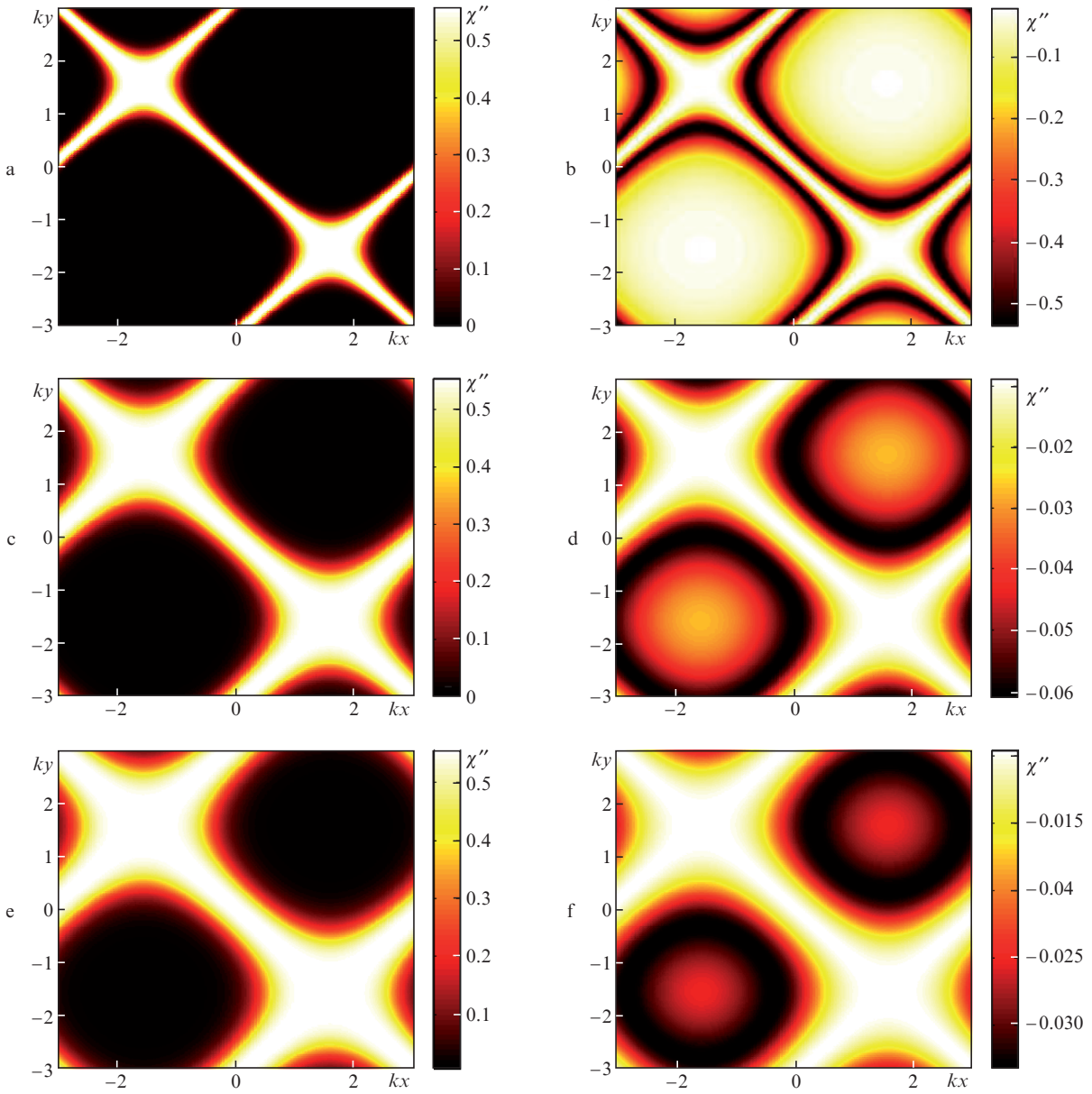

Figure 2. Imaginary part of the susceptibility χ'' as a function of kx, ky at Δ_c = (a, b) 0, (c, d) 10γ, (e, f) 20γ, $\eta_1 = \eta_2$ = (a, c, e) 0 and (b, d, f) 1; γ = 0.1, $\Omega_p = \gamma$, $\Omega_{xy} = 10\gamma$, $\Delta = 2\gamma$ and $\Delta_p = \gamma$.

ings. It can be seen that on resonance, for $\Delta_p = 0$, the probe absorption is distributed in all the quadrants of the xy plane. In this case, with increasing Δ_p, the two cross-like patterns in the second and fourth quadrants will be fading away, and only the spike-like patterns in the first and third quadrants will remain. This is to say that with increasing Δ_p, the absorption peaks move from the second and fourth quadrants to the first and third ones. Physically, quantum interference arising from decay channels leads to enhancement of atomic coherence due to the parallel orientation of the corresponding dipole moments. This leads to precise information about the position of the atom moving through the two-dimensional standing-wave fields. Hence, the position of the atom is determined in sub-wavelength domain.

Figure 4 demonstrates the effect of the intensity of the standing-wave fields on 2D atom localisation. For $\Omega_{xy} = \gamma$ the probe absorption is also distributed in two quadrants of the xy plane (Figs 4a and 4b). With increasing Ω_{xy} from γ and 40γ, the spike-like pattern of Fig. 4a converts to the cross-like pattern (Figs 4c, 4d and Figs 4e, 4f). Thus, for $\eta_1 = \eta_2 = 0$, the intensity of the two standing-wave fields is an important parameter for precise atom localisation. The effect of the intensity of two standing-wave fields for $\eta_1 = \eta_2 = 1$ is displayed in Figs 4b, 4d and 4f. To achieve a better resolution, the intensity of two-orthogonal standing-waves is tuned from 20 to 40γ. It can be seen that the so-called cross-like and spherical-like patterns are also presented, and by increasing the Rabi-frequency of the standing-wave fields, the precision and resolution of the patterns will become better. One can discover where the atom is localised by checking the patterns in the probe absorption spectra. Moreover, the number of the peaks in probe absorption for one period of the standing-wave fields reflects the conditional position probability in the xy plane.

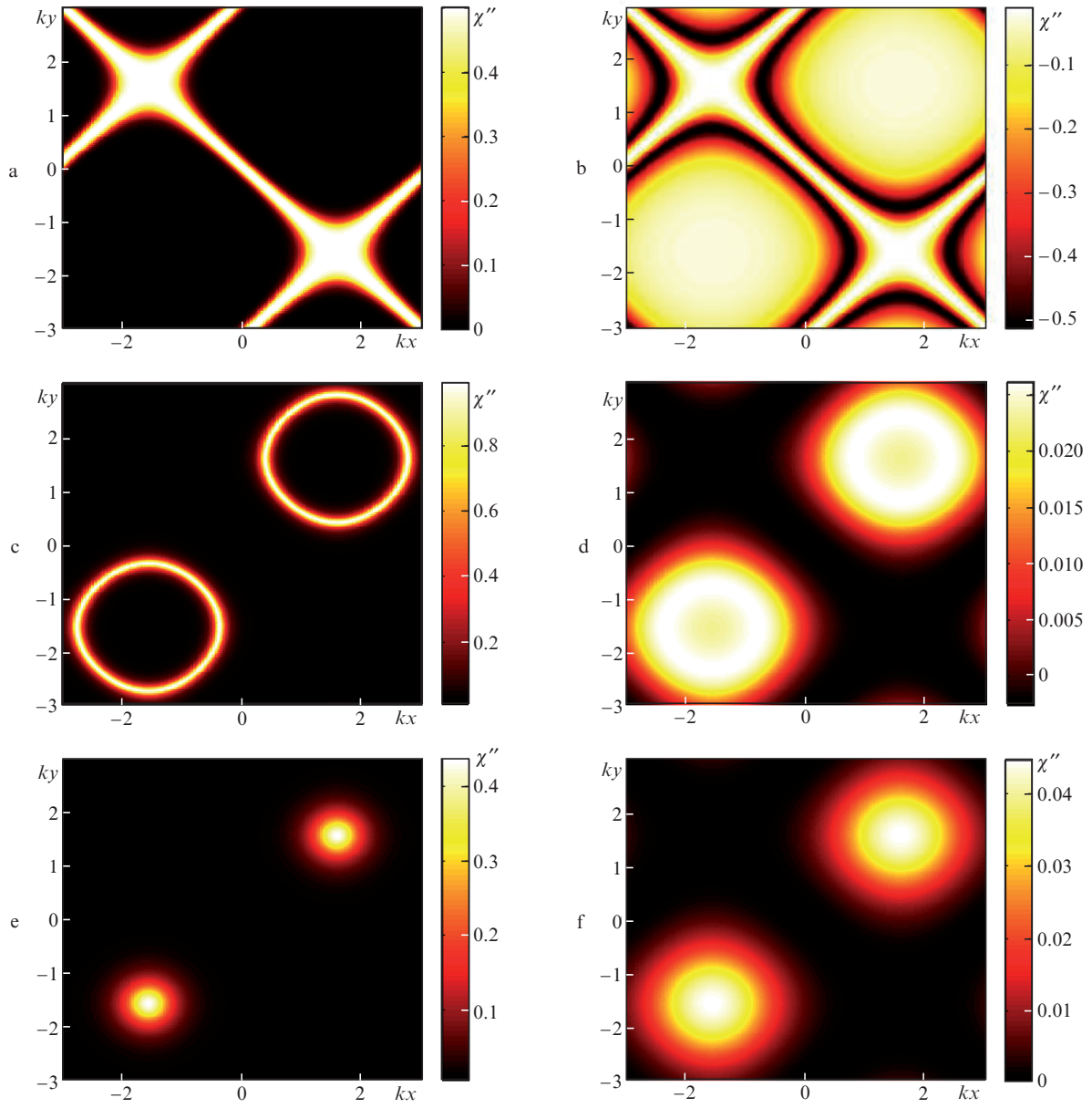

Figure 3. Imaginary part of the susceptibility χ'' as a function of kx, ky at Δ_p = (a, b) 0, (c, d) 20γ, (e, f) 30γ, $\eta_1 = \eta_2$ = (a, c, e) 0 and (b, d, f) 1; γ = 0.1, $\Omega_p = \gamma$, $\Omega_{xy} = 10\gamma$, $\Delta = 2\gamma$ and $\Delta_p = \gamma$.

4. Conclusions

We propose a four-level Λ-type atomic system for two-dimensional atom localisation inside two-orthogonal standing-wave fields. By measuring the probe field absorption, the position probability distribution of the atom is determined in the xy plane. Quantum interferences arising for two decay channels on two-dimensional atom localisation is described. The effect of interaction parameters such as the intensity of standing-waves and the detuning of probe and standing-wave fields, on two-dimensional atom localisation is discussed. Appropriate intensity values of the two orthogonal standing-wave fields lead to precise measurement of the position of an atom moving through the standing-wave fields.

Acknowledgements. This work has been supported by Vice Chancellor for Research and Technology, University of Tabriz, Iran.

References

1. Jin L., Sun H., et al. *J. Mod. Opt*., **56** (6), 805 (2009).
2. Chu S., Wieman C. *J. Opt. Soc. Am. B*, **6** (11), 2020 (1989).
3. Collins G.P. *Phys. Today*, **49** (3), 18 (1996).
4. Qamar S., Zhu S.-Y., et al. *Opt. Commun*., **176** (4), 409 (2000).
5. Qamar S., Zhu S.-Y., et al. *Phys. Rev. A*, **61** (6), 063806 (2000).
6. Ghafoor F., Qamar S., et al. *Phys. Rev. A*, **65** (4), 43819 (2002).
7. Paspalakis E., Knight P.L. *Phys. Rev. A*, **63** (6), 65802 (2001).
8. Tajalli H., Sahrai M. *Laser Phys*., **14** (7), 1007 (2004).
9. Sahrai M. *Laser Phys*., **17** (2), 98 (2007).
10. Sahrai M., Tajalli H., et al. *Phys. Rev. A*, **72** (1), 13820 (2005).
11. Boller K., Imamolu A., Harris S. *Phys. Rev. Lett*., **66** (20), 2593 (1991).
12. Javanainen J. *Europhys. Lett*., **17** (5), 407 (1992).
13. Sahrai M., Tajalli H. *J. Opt. Soc. Am. B*, **30** (3), 512 (2013).
14. Wan R.-G., Kou J., Jiang L., Jiang Y., Gao J.-Y. *J. Opt. Soc. Am. B*, **28** (4), 622 (2011).
15. Wan R.-G., Kou J., et al. *Opt. Commun*., **284** (4), 985 (2011).
16. Lukin M.D., Yelin S.F., et al. *Phys. Rev. A*, **60** (4), 3225 (1999).
17. Ivanov V., Rozhdestvensky Y. *Phys. Rev. A*, **81** (3), 33809 (2010).

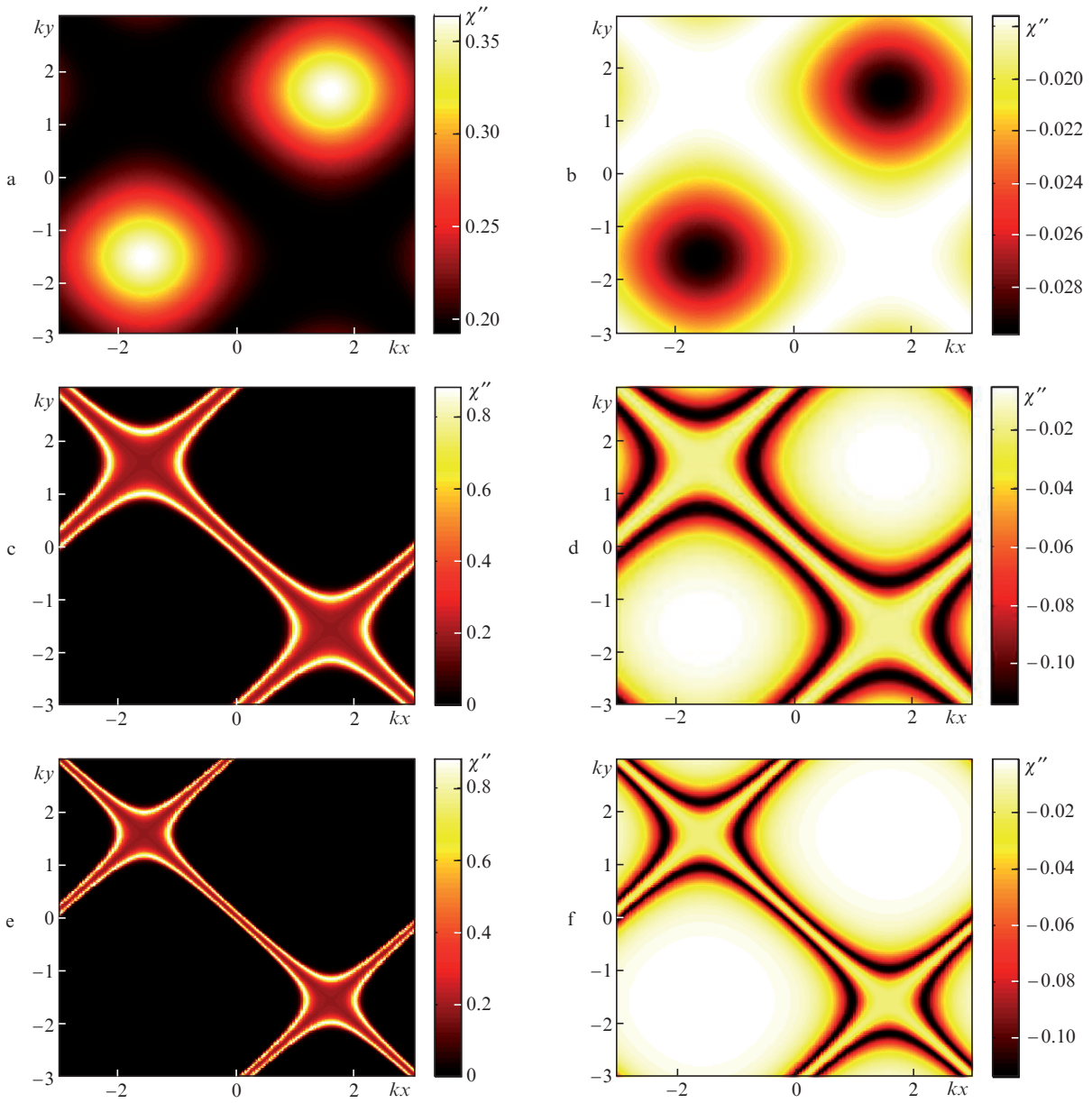

Figure 4. Imaginary part of the susceptibility χ'' as a function of kx, ky at Ω_{xy} = (a, b) γ, (c, d) 20γ, (e, f) 40γ, $\eta_1 = \eta_2$ = (a, c, e) 0 and (b, d, f) 1; γ = 0.1, $\Omega_p = \gamma$, $\Delta = 2\gamma$, $\Delta_c = 0$ and $\Delta_p = 5\gamma$.

18. Li J., Yu R., et al. *Phys. Lett. A*, **375** (45), 3978 (2011).
19. Ding C., Li J., et al. *Phys. Rev. A*, **84** (4), 43840 (2011).
20. Ding C., Li J., et al. *J. Phys. B: At. Mol. Opt. Phys.*, **44** (14), 45501 (2011).
21. Qamar S. *Phys. Rev. A*, **88** (1), 13846 (2013).
22. Shapiro D.A. *JETP*, **88**, 1072 (1999) [*Zh. Eksp. Teor. Fiz.*, **115**, 1961 (1999)].
23. Scully M.O., Zubairy M.S. *Quantum Optics* (Cambridge: Cambridge Univ. Press, 1997).
24. Wang Z., Jiang J. *Phys. Lett. Sect. A: Gen. At. Sol. State Phys.*, **374**, 4853 (2010).